

Psychedelics and schizophrenia: Distinct alterations to Bayesian inference

Hardik Rajpal^{a,b,n,1}, Pedro A.M. Mediano^{c,d,1}, Fernando E. Rosas^{a,e,f}, Christopher B. Timmermann^e, Stefan Brugger^{i,j}, Suresh Muthukumaraswamy^k, Anil K. Seth^{l,m}, Daniel Bor^{c,d}, Robin L. Carhart-Harris^{e,g}, Henrik J. Jensen^{a,b,h}

^aCentre for Complexity Science, Imperial College London, South Kensington, London, United Kingdom

^bDepartment of Mathematics, Imperial College London, South Kensington, London, United Kingdom

^cDepartment of Psychology, University of Cambridge, Cambridge, United Kingdom

^dDepartment of Psychology, Queen Mary University of London, London, United Kingdom

^eCentre for Psychedelic Research, Department of Brain Sciences, Imperial College London, London, United Kingdom

^fData Science Institute, Imperial College London, London, United Kingdom

^gPsychedelics Division, Neuroscape, Department of Neurology, University of California San Francisco, US

^hInstitute of Innovative Research, Tokyo Institute of Technology, Yokohama, Japan

ⁱCardiff University Brain Research Imaging Centre, School of Psychology, Cardiff University, United Kingdom

^jCentre for Academic Mental Health, Bristol Medical School, University of Bristol, United Kingdom

^kSchool of Pharmacy, The University of Auckland, New Zealand

^lSchool of Engineering and Informatics, University of Sussex, United Kingdom

^mCIFAR Program on Brain, Mind, and Consciousness, Toronto, Canada

ⁿPublic Policy Program, The Alan Turing Institute, London, United Kingdom

Abstract

Schizophrenia and states induced by certain psychotomimetic drugs may share some physiological and phenomenological properties, but they differ in fundamental ways: one is a crippling chronic mental disease, while the others are temporary, pharmacologically-induced states presently being explored as treatments for mental illnesses. Building towards a deeper understanding of these different alterations of normal consciousness, here we compare the changes in neural dynamics induced by LSD and ketamine (in healthy volunteers) against those associated with schizophrenia, as observed in resting-state M/EEG recordings. While both conditions exhibit increased neural signal diversity, our findings reveal that this is accompanied by an increased transfer entropy from the front to the back of the brain in schizophrenia, versus an overall reduction under the two drugs. Furthermore, we show that these effects can be reproduced via different alterations of standard Bayesian inference applied on a computational model based on the predictive processing framework. In particular, the effects observed under the drugs are modelled as a reduction of the precision of the priors, while the effects of schizophrenia correspond to an increased precision of sensory information. These findings shed new light on the similarities and differences between schizophrenia and two psychotomimetic drug states, and have potential implications for the study of consciousness and future mental health treatments.

Keywords: Psychedelics, Schizophrenia, Information theory, Predictive processing

1. Introduction

Classic serotonergic psychedelic drugs have seen a blooming resurgence among the public and the scientific community in recent years, largely driven by promising clinical research into their therapeutic potential [1, 2]. At the same time, and somewhat paradoxically, psychedelics are known to elicit effects that mimic some symptoms of psychosis – earning them the label of ‘psychotomimetic drugs’ [3]. Elucidating the similarities and differences between the psychedelic state and schizophrenia is an important neuroscientific challenge that could deepen our understanding of the substantive alterations of perception, cognition, and conscious experience induced by these conditions, while

paving the way towards safe and effective psychedelic therapy.

To contrast these conditions in an empirical manner, we compare neuroimaging data from patients suffering from schizophrenia and healthy subjects under the effects of two psychoactive substances: the classical psychedelic lysergic acid diethylamide (LSD) [4] and the dissociative drug ketamine (KET) [5]. Using standardised assessments, it has been claimed that KET reproduces both positive and negative symptoms of schizophrenia in humans [6], and its mechanism of action – NMDA receptor antagonism – is thought to reproduce a key element of the molecular pathophysiology of schizophrenia [7, 8]. LSD – in common with all classical psychedelics – is a potent agonist of a number of serotonin receptors, but its characteristic effects depend primarily on 5-HT_{2A} [9]. These neurotransmitter systems are linked to psychosis (in particular visual perceptual changes), and are implicated in psychotic disorders

Email addresses: h.rajpal15@imperial.ac.uk (Hardik Rajpal), pam83@cam.ac.uk (Pedro A.M. Mediano)

¹H.R. and P.M. contributed equally to this work.

like schizophrenia – although see Ref. [10] for an alternative account.

Both psychotomimetic drug states and schizophrenia are also associated with marked changes in large-scale neural dynamics. For both LSD and KET, previous studies have found increased signal diversity in subjects' neural dynamics [11, 12] and reduced information transfer between brain regions [13]. However, in the case of KET, evidence from intracranial recordings in cats suggests a much more complicated picture than that of LSD, with very high variability across individuals, brain regions, and dose levels [14]. In a separate line of enquiry, work on EEG data from patients with schizophrenia has also found increased signal diversity [15, 16], akin to the effect found under these drugs. Nonetheless, a parsimonious account explaining the similarities and differences between the two states is still lacking.

A promising approach to gain insights into the mechanisms driving the core similarities and differences between psychotomimetic drug states and schizophrenia is to leverage principles from the predictive processing (PP) framework of brain function [17, 18]. A key postulate of the PP framework is that the dynamics of neural populations can be viewed as engaged in processes of inference involving top-down and bottom-up signals. Under this framework, brain activity can be viewed as resulting from a continuous modelling process in which a prior distribution interacts with new observations via incoming sensory information. In accordance with principles of Bayesian inference, discrepancies between the prior distribution and incoming signals (called 'prediction errors') carried by the bottom-up signals drive revisions to the top-down activity, so as to minimize future surprise.

The PP framework has been used to explain perceptual alterations observed in both psychotomimetic drug states [19, 20] as well as in psychiatric illnesses [21] with a focus on schizophrenia [22, 23, 24, 25]. PP has also been used to understand the action of psychedelics, most notably through the 'relaxed beliefs under psychedelics' (or REBUS) model [26] which posits that psychedelics reduce the precision of prior beliefs encoded in spontaneous brain's activity. REBUS has also been used to inform thinking on the therapeutic mechanisms of psychedelics, where symptomatology can be viewed as pathologically over-weighted beliefs or assumptions encoded in the precision weighting of brain activity encoding them.

To deepen our understanding of the similarities and differences between these conditions, in this paper we replicate and extend findings on neural diversity and information transfer under the two psychotomimetic drugs (LSD and KET) and in schizophrenia using EEG and MEG recordings, and we reproduce these experimental findings as perturbations to a single PP model. Our modelling results reveal that the effects observed under the drugs are indeed reproduced by decreasing the precision-weighting of the priors, while the effects observed under schizophrenia are reproduced by increased precision-weighting of the bottom-

up sensory information. Overall, this study puts forward a more nuanced understanding of the relationship between two different psychotomimetic drug states and schizophrenia, and offers a new model-based perspective on how these conditions alter conscious experience.

2. Materials and Methods

2.1. Data acquisition and preprocessing

Data from 29 patients diagnosed with schizophrenia and 38 age-matched healthy control subjects were obtained from the Bipolar-Schizophrenia Network on Intermediate Phenotypes (BSNIP) database [27]. The subjects were selected within an age range of 20-40 years to match the psychedelic datasets described below. Data included 64-channel EEG recordings sampled at 1000 Hz of each subject in eyes-closed resting state, along with metadata about demographics (age and gender), and patients' medications. The strength of the medication was estimated using the number of antipsychotics taken by each patient (mean: 2.7, range: 0-8), as the dosage of each medication was not available.

Data from healthy subjects under the effects of both drugs was obtained from previous studies with LSD [4] (N = 17) and ketamine [28] (N = 19). Data included MEG recordings from a CTF 275-channel axial gradiometer system with a sampling frequency of 600 Hz. Each subject underwent two scanning sessions in eyes-closed resting state: one after drug administration and another after a placebo (PLA).

Preprocessing steps for all datasets were kept as consistent as possible, and were performed using the Fieldtrip [29] and EEGLAB [30] libraries. First, the data was segmented into epochs of 2 seconds, and epochs with strong artefacts were removed via visual inspection. Next, muscle and eye movement artefacts were removed using ICA [31]. Then, a LCMV beamformer [32] was used to reconstruct activity of sources located at the centroids of regions in the Automated Anatomical Labelling (AAL) brain atlas [33]. Finally, source-level data was bandpass-filtered between 1–100 Hz, and downsampled with phase correction to 250 Hz (EEG) and 300 Hz (MEG), and AAL areas were grouped into 5 major Regions of Interest (ROIs): frontal, parietal, occipital, temporal and sensorimotor (see Figure 1 and Table B.1 in the Appendix). In the rest of the paper we refer to these 5 areas as "ROIs" and to the AAL regions as "sources."

2.2. Analysis metrics

Our analyses are focused on two complementary metrics of neural activity: Lempel-Ziv complexity (LZ) and transfer entropy (TE). Both metrics are widely used and robustly validated measures of neural dynamics across states of consciousness [13, 34, 11, 12].

Lempel-Ziv complexity (LZ) is a measure of the diversity of patterns observed in a discrete – typically binary –

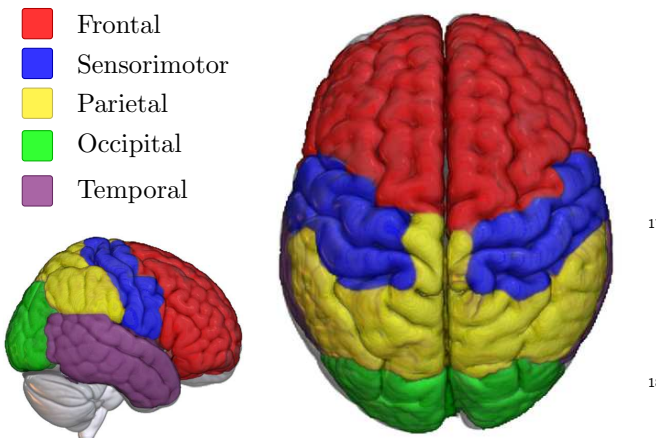


Figure 1: **Regions of interest (ROIs) represented on the MNI-152 standard template.** Each ROI is comprised of several regions of the AAL atlas, as per Table B.1.

sequence. When applied to neuroimaging data, lower LZ (with respect to wakeful rest) has been associated with unconscious states such as sleep [35] or anaesthesia [36], and higher LZ with states of richer phenomenal content [190] under psychedelics, ketamine [11, 12] and states of flow during musical improvisation [37].

To calculate LZ, first one needs to transform a given signal of length T into a binary sequence. For a given epoch of univariate M/EEG data, we do this by calculating [195] the mean value and transforming each data point above the mean to 1 and each point below to 0. Then, the resulting binary sequence is scanned sequentially using the LZ76 algorithm presented by Kaspar and Schuster [38], which counts the number of distinct “patterns” in the [200] signal. Finally, following results by Ziv [39], the number of patterns is divided by $\log_2(T)/T$ to yield an estimate of the signal’s entropy rate [40], which we refer to generically as LZ. This process is applied separately to each source [205] time series (i.e. to each AAL region), and the resulting values are averaged according to the grouping in Table B.1 to yield an average LZ value per ROI.

In addition to LZ, our analyses also consider transfer entropy (TE) [34] — an information-theoretic version of [165] Granger causality [41] — to assess the dynamical interdependencies between ROIs. The TE from a source region to [210] a target region quantifies how much better one can predict the activity of the target after the activity of the source is known. This provides a notion of directed functional connectivity, which can be used to analyse the structure of large-scale brain activity [13, 42].

Mathematically, TE is defined as follows. Denote the [215] activity of two given ROIs at time t by the vectors \mathbf{X}_t and \mathbf{Y}_t , and the activity of the rest of the brain by \mathbf{Z}_t . Note that \mathbf{X}_t , \mathbf{Y}_t , and \mathbf{Z}_t have one component for each AAL source in the corresponding ROI(s). TE is computed in terms of [220] Shannon’s mutual information, I , as the information about the future state of the target, \mathbf{Y}_{t+1} , provided by \mathbf{X}_t over

and above the information in \mathbf{Y}_t and \mathbf{Z}_t :

$$\text{TE}_{Y \rightarrow X|Z} = I(\mathbf{X}_t; \mathbf{Y}_{t+1}^- | \mathbf{X}_{t-1}^-, \mathbf{Z}_{t-1}^-), \quad (1)$$

where \mathbf{X}_t^- refers to the (possibly infinite) past of \mathbf{X}_t , up to and including time t (and analogously for \mathbf{Y}_t and \mathbf{Z}_t). This quantity can be accurately estimated using state-space models with Gaussian innovations [43], implemented using the MVGC toolbox [44]. Note that, when calculating the TE between ROIs, we consider each ROI as a vector — without averaging the multiple AAL sources into a single number. The result is a directed 5×5 network of conditional TE values between pairs of ROIs, which can be tested for statistical differences across groups.

2.3. Statistical analysis

For both LSD and KET datasets, since the same subjects were monitored under both drug and placebo conditions, average subject-level differences (either in LZ or TE) were calculated for each subject, and one-sample t-tests were used on those differences to estimate the effect of the drug.

For the data of patients and controls in the schizophrenia dataset, group-level differences were estimated via linear models. These models used either LZ or TE as target variable, and condition (schizophrenia or healthy), age, gender, and number of antipsychotics (set to zero for healthy controls) as predictors. Motivated by previous work suggesting a quadratic relationship between complexity and age [45], each model was built with either a linear or quadratic dependence on age, and the quadratic model was selected if it was preferred over a linear model by a log-likelihood ratio test (with a critical level of 0.05).

Finally, multiple comparisons when comparing TE values across all pairs of ROIs were addressed by using the Network-Based Statistic (NBS) [46] method, which identifies ‘clusters’ of differences — i.e. connected components where a particular null hypothesis is consistently rejected while controlling for family-wise error rate. Our analysis used an in-house adapted version of NBS that works on directed networks, such as the ones provided by TE analyses.

2.4. Computational modelling

A computational model was developed in order to interpret the LZ and TE findings observed on the neuroimaging data. Building on *predictive processing* principles [18], we constructed a Bayesian state-space model that provides an idealised common ground to contrast the three studied conditions — the psychotomimetic drug states, schizophrenia, and baseline (i.e. healthy controls). Our modelling is based on the postulate that the activity of neuronal populations across the brain can be interpreted as carrying out inference on the causes of their afferent signals. Following this view, the proposed model considers the following elements:

- the internal state of a low-level region (i.e. near the sensory periphery), denoted by s_t ;

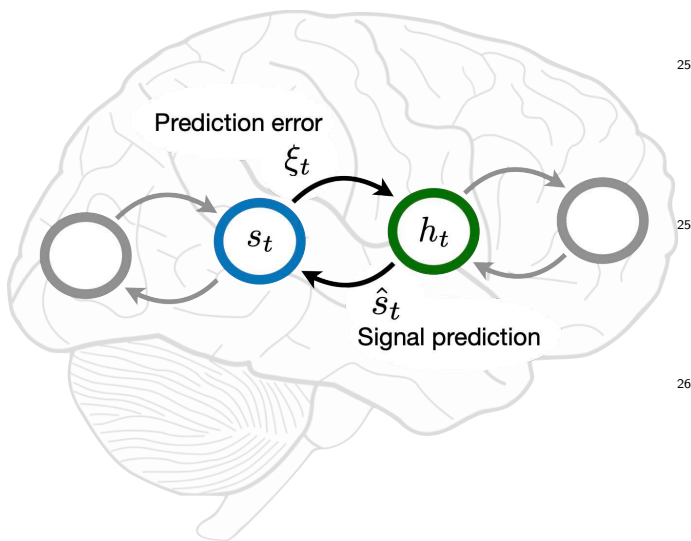


Figure 2: **Graphical illustration of the predictive processing model.** The activity of a high-level neural population is represented as a prediction \hat{s}_t , and the activity of a low-level population as a prediction error ξ_t . The internal states of the high- and low-level regions are captured by s_t and h_t , respectively.

- the internal state of neural activity taking place functionally one level above, denoted by h_t ;
- the signal generated at the high-level region in the form of a prediction of the low-level activity, denoted by \hat{s}_t ;
- the signal generated at the low-level region in the form of a prediction error ξ_t ; and
- the precision of the prior λ_p and precision of sensory/afferent information λ_s .

This model represents neural activity within a larger hierarchical processing structure, as illustrated in Figure 2. The key principle motivating this model is that minimisation of prediction error signals throughout the hierarchy, by updating top-down predictions, implements a tractable approximation to Bayesian inference.²

Within this model, we represent the schizophrenia and psychedelic conditions as different types of disruption to Bayesian inference. To describe the psychedelic state, we build on the REBUS hypothesis [26], which posits a reduced precision-weighting of prior beliefs, leading to increased bottom-up influence. Conversely, to describe schizophrenia we build on the canonical predictive processing account of psychosis in schizophrenia [48], which postulates an increased precision of sensory input, along with decreased precision of prior beliefs [22, 21]. Therefore, both conditions are similar in that there is a relative strengthening of

²Note that in the simple scenario of Eqs. (3), with a single level and Gaussian distributions, inference is in fact exact. In larger or more complicated models inference is often carried out only approximately [47].

bottom-up influence, although instantiated in different ways – which, as shown in Sec. 3.3, bears important consequences for the behaviour of the model.

It is important to note that predictive processing accounts of schizophrenia remain hotly debated, with other works proposing an increase of prior precision (instead of decrease) as a model of auditory and visual hallucinations [49, 50]. Recent reviews [48] have attempted to reconcile both views by suggesting that sensory hallucinations may be caused by stronger priors, while hallucinations related to self-generated phenomena (like inner speech or self-attention [51]) may stem from weaker priors. Here, we base our modelling of SCZ on the weak prior hypothesis, as described above – we return to this issue in this discussion.

To simulate the aberrant dynamics of the inference process, as described above, we consider a given afferent signal (s_t) and construct the corresponding activity of a higher area (h_t), prediction (\hat{s}_t), and prediction error (ξ_t), building on the rich literature of state-space models in neuroscience [52, 53, 54]. Specifically, we use the linear stochastic process:

$$h_t = ah_{t-1} + \epsilon_t \quad (2a)$$

$$s_t = bh_t + \nu_t, \quad (2b)$$

where a, b are weights, and ϵ_t, ν_t are zero-mean Gaussian terms with precision (i.e. inverse variance) λ_p and λ_s , respectively. Note that this formulation is equivalent to

$$h_t|h_{t-1} \sim \mathcal{N}(ah_{t-1}, \lambda_p^{-1}), \quad (3a)$$

$$s_t|h_t \sim \mathcal{N}(bh_t, \lambda_s^{-1}). \quad (3b)$$

As we show in the following, λ_p corresponds to the precision of the prior and λ_s to the precision of sensory/afferent information.

The dynamics of this system can be described as a recurrent update between predictions and prediction errors as follows. Eq. (3b) implies that the internal state h_t generates a prediction about the low-level activity given by $\hat{s}_t = bh_t$. At the same time, the dynamics of the high-level region can be seen as a Bayesian update of h_t given s_t and h_{t-1} . Under some simplifying assumptions, the mean of the posterior distribution of h_{t+1} (denoted by \hat{h}_{t+1}) is equal to (see Appendix A)

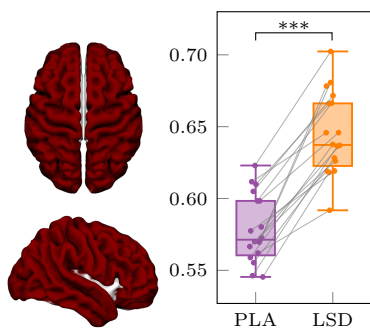
$$\hat{h}_{t+1} = a\hat{h}_t + \beta\xi_t, \quad (4)$$

which effectively combines a *prior* $a\hat{h}_t$ (which is the optimal prediction of h_{t+1} given only \hat{h}_t , as seen from Eq. (3a)) and a *likelihood* given by the prediction error $\xi_t = s_t - \hat{h}_t$ that is precision-weighted via β , a parameter known as the *Kalman gain* [55].

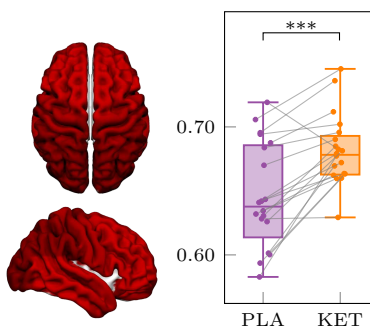
In our simulations, the model is first calibrated using as afferent signals (i.e. s_t) data from the primary visual cortex, corresponding to epochs randomly sampled from the placebo conditions in the LSD and KET datasets. This calibration results in the estimation of the model parameters $a^{\text{con}}, b^{\text{con}}, \lambda_p^{\text{con}}, \lambda_s^{\text{con}}$ for the control condition, which

Psychotomimetic drugs

LSD - PLA



KET - PLA



Schizophrenia

SCZ - CTRL

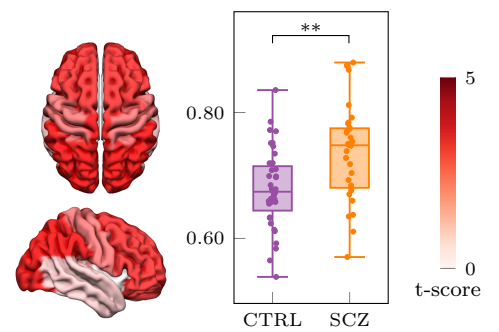


Figure 3: **Increased signal diversity in subjects under the effects of psychotomimetic drugs and in schizophrenia patients.** LZ changes are widespread across all ROIs in the three datasets. For the schizophrenia dataset, LZ values shown are corrected for age, gender, and the number of antipsychotic medications taken by each patient using a linear model.

is done using the well-known expectation-maximisation algorithm [56]. With these, the schizophrenia condition is then modelled by setting

$$\lambda_p^{scz} = \lambda_p^{\text{con}} \quad \text{and} \quad \lambda_s^{scz} = \eta \lambda_s^{\text{con}}, \quad (5)$$

where $\eta > 1$ is referred to as a *noise factor*. This increase of λ_s induces a strengthening of bottom-up prediction errors, and makes the posterior of h_t excessively precise. Conversely, the drug condition is modelled by setting

$$\lambda_p^{\text{psy}} = \frac{\lambda_p^{\text{con}}}{\eta} \quad \text{and} \quad \lambda_s^{\text{psy}} = \lambda_s^{\text{con}}. \quad (6)$$

Reducing λ_p also increases the influence of prediction errors, but reduces the precision of the posterior of h_t . Subsequently, for both conditions the parameters a, b are re-trained with another pass of the expectation-maximisation algorithm on the placebo trials.

Finally, to compare the model with the empirical M/EEG data, the LZ of the neural activity elicited in the low-level area (i.e. the prediction errors, ξ_t) and the top-down transfer entropy (from the high-level activity \hat{s}_t towards the low-level activity ξ_t) are calculated for each of these three models (control, schizophrenia, and drug).

3. Results

3.1. LSD, KET and schizophrenia all show increased LZ

We begin the analysis by comparing changes in signal diversity, as measured by LZ, across the LSD, ketamine (KET), and schizophrenia (SCZ) datasets.

Our results show strong and significant increases in LZ in all three datasets (Fig. 3), in line with previous work [11, 12, 15, 16]. In all three cases the LZ increases are widespread throughout the brain, with the effects in schizophrenia patients being more pronounced in frontal and parietal regions. While the t-scores are higher in LSD

and KET than schizophrenia, this could be due to the within-subjects design of both drug experiments – which are more statistically powerful than the between-subjects analysis used on the schizophrenia dataset.

Interestingly, we found that controlling for the medication status of each schizophrenia patient was crucial to obtain results that match prior work [15]. A direct comparison of LZ values between patients and controls yielded no significant differences ($t = -0.38, p = 0.70$); however, when using a linear model correcting for age, gender, and number of antipsychotics, the antipsychotics coefficient of the model reveals a negative effect on LZ ($\beta = -0.016, t = -2.3, p = 0.021$). Additionally, a two-sample t-test calculated between the corrected LZ values of patients and controls yields a substantial difference ($t = 3.4, p = 0.001$). Nonetheless, the sensitivity of this result to these pre-processing steps means it should be considered preliminary and explored further in future research (see the corresponding discussion in Sec. 4.3).

3.2. Opposite effect of psychotomimetic drugs and schizophrenia on information transfer

We next report the effects of LSD, KET, and schizophrenia on large-scale information flow in the brain, as measured via transfer entropy (TE). The TE between each pair of ROIs (conditioned on all other ROIs) is calculated for each subject, and used to build directed TE networks. The resulting networks were tested for differences between the drug states and placebo conditions (for LSD and KET), and between patients and controls (for SCZ), correcting for multiple comparisons via cluster permutation testing (see Sec. 2.3).

We found a ubiquitous decrease in the TE between most pairs of ROIs under LSD and KET (Fig. 4), which is consistent with previous findings [13]. In contrast, SCZ patients exhibit marked localised increases in TE – and no decreases – with respect to the control subjects. Notably,

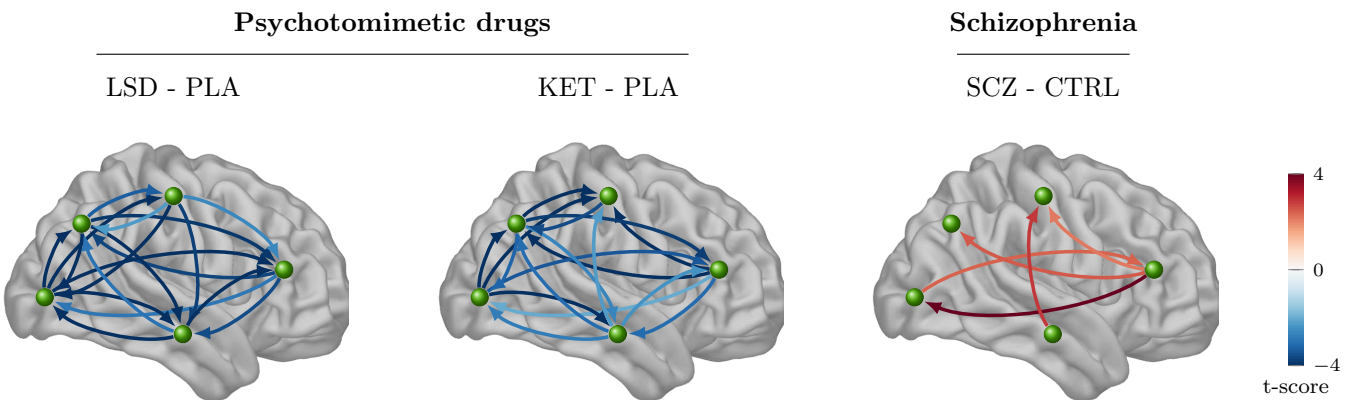


Figure 4: **Lower information transfer under LSD and ketamine but higher information transfer for schizophrenia patients.** Transfer entropy (TE) shows a strong widespread decrease in subjects under the effect of LSD or ketamine (KET), compared to a placebo. Conversely, schizophrenia (SCZ) patients show an increase in TE with respect to controls (CTRL), especially from the frontal region to the rest of the brain (controlling for age, gender and antipsychotic use). Links shown are significant after multiple comparisons correction.

most increases in TE originated in the frontal ROI, and are strongest between the frontal and occipital ROIs. The increase of information transfer seen in schizophrenia patients therefore takes place “front to back” – aligned with the pathways thought to carry top-down information in the brain from highly cognitive, decision-making regions to unimodal regions closer to the sensory periphery.

As was the case for LZ, controlling for antipsychotic use was key to revealing differences between the healthy controls and schizophrenia patients. In addition, we found a small negative correlation between antipsychotic use and TE between certain ROI pairs – but, unlike for LZ, this effect did not survive correction for multiple comparisons.

3.3. Computational model reproduces experimental results

So far, we have seen that subjects under the effects of two different psychotomimetic drugs display increased signal diversity and reduced information flow in their neural dynamics. In comparison, schizophrenia patients display increased complexity but also increased information flow with respect to healthy controls. We now show how complementary perturbations to the precision terms of the predictive processing model introduced in Section 2.4 reproduce these findings.

We compared the baseline model against the drug and schizophrenia variants by systematically increasing the noise factor η , which results in reduced prior precision in the drug model, and increased sensory precision in the schizophrenia model. We then computed the corresponding LZ and TE based on the model-generated time series ξ_t , \hat{s}_t as per Sec. 2.4 (Fig. 5).

Results show that the proposed model successfully reproduced the experimental findings of both LZ and TE under the two different psychotomimetic drugs and schizophrenia (Fig. 5). Interestingly, the model also shows (Fig. 5b) that a relative strengthening of sensory information (via either increased sensory precision, or decreased prior precision) can trigger either an increase or a decrease (respectively)

of top-down transfer entropy. This suggests that transfer entropy changes cannot be directly interpreted as revealing the changes in any underlying predictive processing mechanisms (see Discussion).

Finally, as a control, we repeated the analysis on the model but exploring the variation of the precision terms in the two unexplored directions — either reducing λ_p or increasing λ_s (see Section 2.4). Neither of these changes reproduced the experimental findings (results not shown), which highlights the specificity of the modelling choices.

4. Discussion

In this paper we have analysed MEG data from healthy subjects under the effects of the psychotomimetic drugs LSD and ketamine, as well as EEG data from a cohort of schizophrenia patients and healthy control subjects. We focused on signal diversity and information transfer, both widely utilised metrics of neural dynamics. We found that all datasets show increases in signal diversity, but diverging changes in information transfer, which was higher in schizophrenia patients but lower for subjects under the effects of either drug. In addition to replicating previous results reporting signal diversity and information transfer under the effects of both drugs [11, 12, 13], we described new findings applying these metrics to schizophrenia.

Using a computational model inspired by predictive processing principles [18, 57], we showed that this combination of effects can be reproduced via specific alterations to prediction updating, which can be interpreted as specific forms of disruption to Bayesian inference. Critically, the effects of both psychotomimetic drugs and schizophrenia, on both signal diversity and information transfer, are explained by a relative strengthening of sensory information over prior beliefs, although triggered by different mechanisms – a decrease in the precision of priors in the case of psychotomimetic drugs (consistent with Ref. [26]), and

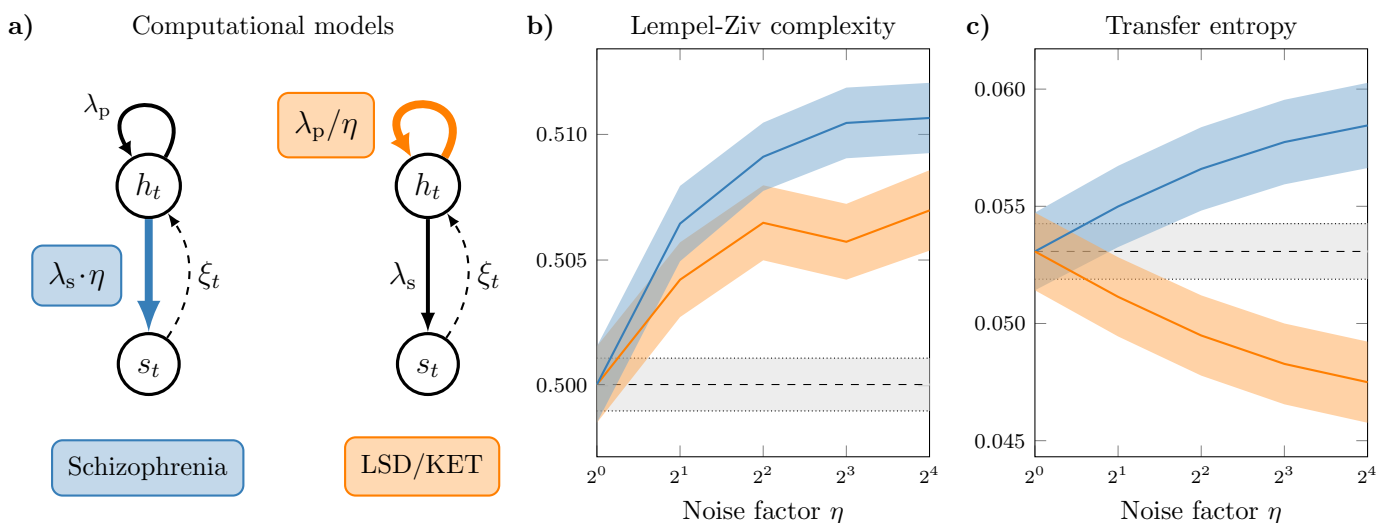


Figure 5: **A computational model based on predictive processing principles reproduces experimental findings in the LSD, ketamine and schizophrenia datasets.** (a) By increasing the sensory precision (for schizophrenia; blue), or reducing the prior's precision (for LSD and KET; orange) by a given 'noise' factor η , the model can reproduce the experimental findings of (b) increased in LZ in both conditions, and (c) opposite changes in TE in both conditions, compared to a baseline (grey).

an increase in the precision of sensory information for₄₃₅ schizophrenia.

4.1. Increased sensory precision in schizophrenia

The idea that the symptoms of schizophrenia can be understood as alterations to processes of Bayesian inference has been particularly fertile in the field of computational psychiatry [21]. In particular, various studies based on PP have related psychosis to decreased precision of prior beliefs and increased precision of the sensory inputs [58, 19, 22, 59, 60]. These computational models have been supported by a growing number of related experimental findings, including an enhanced confirmation bias [61], impaired reversal learning [62, 63], and a greater resistance to visual illusions [64]. For instance, schizophrenia patients are less susceptible to the Ebbinghaus illusion, which arises primarily from misleading prior expectations, suggesting that patients do not integrate this prior context with sensory evidence and thus achieve more accurate judgements [65].

Most of the above mentioned studies are task-based, focusing on differentiating perceptual learning behaviours between healthy controls and schizophrenia patients. Though these studies provide a range of experimental markers, the corresponding methodologies cannot be applied to resting-state or task-free conditions, under which it is known that certain behavioural alterations (e.g. delusions, anhedonia, and paranoia) persist [66, 67].

The findings presented in this paper provide a step towards bridging this important knowledge gap by providing empirical and theoretical insights into resting-state neural activity under schizophrenia. Although we build on and replicate results related to signal diversity, we are not aware of previous studies of information transfer on schizophrenia in resting state.

4.2. Beyond unidimensional accounts of top-down vs bottom-up processing

The findings presented here link spontaneous brain activity to the PP framework using empirical metrics of signal diversity and information transfer. In the psychotomimetic drug condition, the former increases while the latter decreases; in schizophrenia, both increase – in both cases as compared to baseline placebo or control. The explanation for this pattern of results, articulated by our computational model, is based on the idea that a bias favouring bottom-up over top-down processing can be triggered by changing different precision parameters, which can give rise to opposite effects in specific aspects of the neural dynamics. This observation, we argue, opens the door to more nuanced analyses for future studies.

The increased transfer entropy from frontal to posterior brain areas observed under schizophrenia could be naively interpreted as supporting increased top-down regulation; however, neither the empirical analysis nor the computational model warrant this conclusion. Transfer entropy simply indicates information flow and is agnostic about functional role. Moreover, our model-based analyses illustrate how aberrant Bayesian inference in which bottom-up influences become strong can trigger either an increase or a decrease in transfer entropy from frontal to posterior regions, depending on which precision terms are involved. An interesting possible explanation for this divergence between mechanisms and TE is provided by recent results that show that TE is an aggregate of qualitatively different *information modes* [68]. Future work may explore if resolving TE into its finer constituents might provide a more informative mapping from observed patterns to underlying mechanisms.

Taken together, these findings suggest that conceiv-

ing the bottom-up vs top-down dichotomy as a single-⁵²⁵ dimensional trade-off might be too simplistic, and that multi-dimensional approaches could shed more light on this issue. In particular, our results show how such a simplistic view fails to account for the rich interplay of similarities and differences between schizophrenia and psychosis. ⁵³⁰

475 4.3. Limitations and future work

While our empirical and modelling results agree with the canonical PP account of psychosis [48], some reports have suggested a stronger influence of priors over sensory signals⁵³⁵ – especially in some cases of hallucinations [69, 70, 71]. It is important to remark that the ‘strengthened prior’ interpretation put forward by these task-based studies cannot be accounted for by the simple computational modelling developed here. Future work on multi-level extensions of⁵⁴⁰ this model could test if a richer hierarchical model could implicate a stronger influence of certain high-level priors under certain conditions.

Regarding the empirical analyses, it is important to note that our analyses are subject to a few limitations due to the nature of the data used. First, the analyses used only⁵⁴⁵ 60 AAL sources across 5 ROIs (due to the spatial resolution limitations of EEG), and therefore may neglect potential PP effects that may exist at smaller spatial scales. In addition, the studies on both drugs and schizophrenia used different imaging methods (MEG vs EEG), sampling rate⁵⁵⁰ and experiment designs (within vs between subjects), complicating direct comparisons. Finally, future work should examine how power spectra across the different conditions relate to the findings presented, in terms of both their effect on LZ [72], and their relationship with top-down⁵⁵⁵ and bottom-up signalling, for example using band-limited Granger causality [73], as well as how directed functional connectivity measures relate to undirected measures such as mutual information and coherence [13].

Similarly, while the measures discussed here capture⁵⁶⁰ significant differences between schizophrenia patients and healthy controls, more work needs to be done to further characterise the differences within the schizophrenia spectrum, which features a heterogenous array of symptoms and states, e.g. at different phases of the so-called ‘psychotic⁵⁶⁵ process’ [74]. This might entail a closer look at the clinical symptom scores of the patients and their relationship to neural dynamics, which was not possible here due to the lack of appropriate metadata. An interesting possibility is that the neural underpinnings of positive and negative⁵⁷⁰ symptoms could be different [22], and investigating these differences may yield further insight into schizophrenia itself and its relationship with the psychotomimetic drug states. Moreover, both schizophrenia and drug-induced states can be conceived of as dynamic states of consciousness, comprised of several sub-states and/or episodes with⁵⁷⁵ hallucinations, delusions and negative symptoms varying widely between and within individuals. Future studies could explore these finer fluctuations in conscious state [75], as well as what features or episodes overlap in the neural

and psychological levels between psychotomimetic drug states and schizophrenia.

Finally, recall that (as described in Sec. 2.1) we used the number of antipsychotic medications being used by each patient as a proxy measure for their medication load. We acknowledge that this is an oversimplification, and that richer datasets may allow a more detailed inspection of the effects of each particular medication – which would potentially bring more nuance to these analyses. Also, the models used for statistical analysis (as per Sec. 2.3) are linear and may not capture possible non-linear dependencies between antipsychotic use and its effect on neural dynamics (in our case, LZ or TE). Bearing this caveat in mind, the preliminary results regarding antipsychotic use suggest that they bring the patients’ neural dynamics closer to the range of healthy controls. This finding should be replicated with more detailed analyses, and, if robust, could potentially be used to investigate the mechanism of action of current antipsychotic drugs.

485 4.4. Final remarks

In this paper we have contrasted changes in brain activity in individuals with schizophrenia (compared to healthy controls) with changes induced by a classic 5-HT_{2A} receptor agonist psychedelic, LSD, and an NMDA antagonist dissociative, ketamine (compared to placebo). Empirical analyses revealed that both schizophrenia and drug states show an increase in neural signal diversity, but they have divergent transfer entropy profiles. Furthermore, we proposed a simple computational model based on the predictive processing framework [18] that recapitulates the empirical findings through distinct alterations to optimal Bayesian inference. In doing so, we argued that both schizophrenia and psychotomimetic drugs can be described as inducing a stronger “bottom-up” influence of sensory information, but in qualitatively different ways, thus painting a more nuanced picture of the functional dynamics of predictive processing systems. Crucially, the proposed model differs from others in the literature in that it is a model of resting-state (as opposed to task-based) brain activity, bringing this methodology closer to other approaches to neuroimaging data analysis based on complexity science [76].

Overall, this study illustrates the benefits of combining information-theoretic analyses of experimental data and computational modelling, as integrating datasets from patients with those from healthy subjects. We hope our findings will inspire further work deepening our understanding about the relationship between neural dynamics and high-level brain functions, which in turn may accelerate the development of novel, mechanism-based treatments to foster and promote mental health.

520 Acknowledgements

H.R. is supported by the Imperial College President’s PhD Scholarship. P.M. and D.B. are funded by the Wellcome Trust (grant no. 210920/Z/18/Z). F.R. is supported

580 by the Ad Astra Chandaria foundation. C.T. is funded by the Psychedelic Research Group, Imperial College London. R.C.-H. is the Ralph Metzner Chair of the Psychedelic₆₁₀ Division, Neuroscape at University of California San Francisco. A.K.S. is supported by the European Research Council (Advanced Investigator Grant 101019254.) This work 585 was supported in part by grant MR/N0137941/1 for the GW4 BIOMED MRC DTP, awarded to the Universities₆₁₅ of Bath, Bristol, Cardiff and Exeter from the Medical Research Council (MRC)/UKRI (S.B.). The LSD research described here was supported by the Beckley Foundation 590 and Walacea Crowd Funding campaign. We thank Imperial College London's Research Computing Service for the computing facilities. Parts of this work were carried out using₆₂₀ the computational facilities of the Advanced Computing Research Centre, University of Bristol.

595 **Appendix A. Further details on the predictive processing model**

600 This appendix outlines how a process of Bayesian inference on the probability distribution described by Eq. (3) can be interpreted in terms of the joint dynamics of prediction and prediction error. This is covered in standard textbooks of time series analysis (e.g. in Ref. [55]) – however, it is provided here for completeness and accessibility.

As a starting point, we assume that a given brain region is trying to infer the hidden cause h_t of its afferent signal, s_t . The brain can use all the previous signals, $\mathbf{s}^{t-1} = (s_1, \dots, s_{t-1})$, to generate an optimal prior estimation of h_t , which is given by $p(h_t|\mathbf{s}^{t-1})$. When a new sample s_t is observed, this prior can be updated using Bayes' rule, 625

$$p(h_t|\mathbf{s}^t) = \frac{p(h_t, s_t, \mathbf{s}^{t-1})}{p(s_t, \mathbf{s}^{t-1})} = \frac{p(s_t|h_t)p(h_t|\mathbf{s}^{t-1})}{p(s_t|\mathbf{s}^{t-1})}.$$

630 Note that, while in general computing $p(h_t|\mathbf{s}^t)$ can be computationally challenging, when all the distributions in the right-hand side of the equation above are Gaussian (as per Eq. (3)) the posterior is easily calculable – as we explain below. 635

For consistency with the model in Eq. (2), we assume that $h_t|\mathbf{s}^{t-1}$ is a Gaussian random variable with mean \hat{h}_t and variance λ_t^{-1} . By considering $p(h_t|\mathbf{s}^{t-1})$ as a prior and $p(s_t|h_t)$ as a likelihood, we can compute the posterior $p(h_t|\mathbf{s}^t)$ by using Bayes' rule above for Gaussian variables. In this case, standard results for conditional Gaussian distributions (e.g. Ref. [55, Eq. (4.2)]) show that 645

$$\mathbb{E}[h_t|\mathbf{s}^t] = \hat{h}_t + \lambda_t^{-1}bF_t^{-1}\xi_t, \quad (\text{A.1})$$

650 where $\xi_t = s_t - \mathbb{E}[s_t|\mathbf{s}^{t-1}] = s_t - \hat{h}_t$ is the error in the prediction of s_t given \mathbf{s}^{t-1} , and $F_t = b^2\lambda_t^{-1} + \lambda_s^{-1}$ is the predictive covariance of s_t given \mathbf{s}^{t-1} . Then, by using Eq. (3a), one can propagate the prediction in Eq. (A.1) to the next step, and obtain a recurrent update equation for \hat{h}_t given by 655

$$\hat{h}_{t+1} := \mathbb{E}[h_{t+1}|\mathbf{s}^t] = a\mathbb{E}[h_t|\mathbf{s}^t] = a\hat{h}_t + \beta_t\xi_t, \quad (\text{A.2})$$

where $\beta_t = ab\lambda_t^{-1}F_t^{-1}$ is known as the *Kalman gain* parameter [55, Sec. 4.3] and which, as described in Sec. 2.4, depends only on its previous value \hat{h}_{t-1} and the prediction error ξ_t .

Furthermore, from the definition of β_t and F_t it can be seen that increasing λ_s leads to a higher β_t , thus increasing the bottom-up influence of prediction errors. A similar argument can be made for the increase of β_t with lower λ_p , although this requires writing a recurrent expression analogous to Eq. (A.2) for λ_t and is more mathematically involved. Interested readers are referred to Sec. 4.3 of Ref. [55] for a detailed derivation.

Appendix B. Table with definition of the selected ROIs

ROI	AAL indices
Frontal	3-16, 19-20, 23-26
Occipital	43-54
Parietal	59-70
Sensorimotor	1-2, 17-18, 57-58
Temporal	81-90

Table B.1: Selected regions from the AAL atlas and their corresponding region of interest (ROI).

References

- [1] R. L. Carhart-Harris, L. Roseman, M. Bolstridge, L. Demetriou, J. N. Pannekoek, M. B. Wall, M. Tanner, M. Kaelen, J. McGonigle, K. Murphy, et al., Psilocybin for treatment-resistant depression: fMRI-measured brain mechanisms, *Scientific Reports* 7 (1) (2017) 1–11.
- [2] R. L. Carhart-Harris, B. Giribaldi, R. Watts, M. Baker-Jones, A. Murphy-Beiner, R. Murphy, J. Martell, A. Bleatings, D. Erritzoe, D. J. Nutt, Trial of psilocybin versus escitalopram for depression, *New England Journal of Medicine* 384 (15) (2021) 1402–1411.
- [3] R. L. Carhart-Harris, M. Kaelen, M. Bolstridge, T. Williams, L. Williams, R. Underwood, A. Feilding, D. J. Nutt, The paradoxical psychological effects of lysergic acid diethylamide (LSD), *Psychological Medicine* 46 (7) (2016) 1379–1390. doi: 10.1017/S0033291715002901.
- [4] R. L. Carhart-Harris, S. Muthukumaraswamy, L. Roseman, M. Kaelen, W. Droog, K. Murphy, E. Tagliazucchi, E. E. Schenck, T. Nest, C. Orban, et al., Neural correlates of the LSD experience revealed by multimodal neuroimaging, *Proceedings of the National Academy of Sciences* 113 (17) (2016) 4853–4858.
- [5] J. Frohlich, J. D. Van Horn, Reviewing the ketamine model for schizophrenia, *Journal of Psychopharmacology* 28 (4) (2014) 287–302.
- [6] K. Beck, G. Hindley, F. Borgan, C. Ginestet, R. McCutcheon, S. Brugger, N. Driesen, M. Ranganathan, D. C. D’Souza, M. Taylor, et al., Association of ketamine with psychiatric symptoms and implications for its therapeutic use and for understanding schizophrenia: a systematic review and meta-analysis, *JAMA network open* 3 (5) (2020) e204693–e204693.
- [7] K. Friston, H. R. Brown, J. Siemerikus, K. E. Stephan, The dysconnection hypothesis (2016), *Schizophrenia research* 176 (2–3) (2016) 83–94.
- [8] R. A. McCutcheon, J. H. Krystal, O. D. Howes, Dopamine and glutamate in schizophrenia: biology, symptoms and treatment, *World Psychiatry* 19 (1) (2020) 15–33.

[9] D. E. Nichols, Hallucinogens, *Pharmacology & therapeutics* 101 (2) (2004) 131–181. 730

[10] R. L. Carhart-Harris, S. Brugger, D. Nutt, J. Stone, Psychiatry's next top model: Cause for a re-think on drug models of psychosis and other psychiatric disorders, *Journal of Psychopharmacology* 27 (9) (2013) 771–778. doi:10.1177/0269881113494107.

[11] M. M. Schartner, R. L. Carhart-Harris, A. B. Barrett, A. K. Seth, S. D. Muthukumaraswamy, Increased spontaneous MEG signal diversity for psychoactive doses of ketamine, LSD and psilocybin, *Scientific Reports* 7 (2017) 46421. 735

[12] P. A. Mediano, F. E. Rosas, C. Timmermann, L. Roseman, D. J. Nutt, A. Feilding, M. Kaelen, M. L. Kringelbach, A. B. Barrett, A. K. Seth, et al., Effects of external stimulation on psychedelic state neurodynamics, *bioRxiv* (2020). doi:10.1101/2020.11.01.356071.

[13] L. Barnett, S. D. Muthukumaraswamy, R. L. Carhart-Harris, A. K. Seth, Decreased directed functional connectivity in the psychedelic state, *NeuroImage* 209 (2020) 116462. 740

[14] C. Pascovich, S. Castro-Zaballa, P. A. Mediano, D. Bor, A. Canales-Johnson, P. D. Torterolo, T. A. Bekinschtein, Ketamine and sleep modulate neural complexity dynamics in cats, *bioRxiv* (2021). doi:10.1101/2021.06.25.449513. 745

[15] A. Fernández, M.-I. López-Ibor, A. Turrero, J.-M. Santos, M.-D. Morón, R. Hornero, C. Gómez, M. A. Méndez, T. Ortiz, J. J. López-Ibor, Lempel-Ziv complexity in schizophrenia: A MEG study, *Clinical Neurophysiology* 122 (11) (2011) 2227–2235.

[16] Y. Li, S. Tong, D. Liu, Y. Gai, X. Wang, J. Wang, Y. Qiu, Y. Zhu, 750 Abnormal EEG complexity in patients with schizophrenia and depression, *Clinical Neurophysiology* 119 (6) (2008) 1232–1241.

[17] A. Clark, *Surfing uncertainty: Prediction, action, and the embodied mind*, Oxford University Press, 2015.

[18] R. P. Rao, D. H. Ballard, Predictive coding in the visual cortex: 755 A functional interpretation of some extra-classical receptive-field effects, *Nature Neuroscience* 2 (1) (1999) 79–87. doi:10.1038/4580.

[19] P. R. Corlett, C. D. Frith, P. C. Fletcher, From drugs to deprivation: A Bayesian framework for understanding models of psychosis, *Psychopharmacology* 206 (4) (2009) 515–530.

[20] P. Leptourgos, M. Fortier-Davy, R. Carhart-Harris, P. R. Corlett, D. Dupuis, A. L. Halberstadt, M. Kometer, E. Kozakova, F. Laroi, T. N. Noorani, K. H. Preller, F. Waters, Y. Zaytseva, R. Jardri, Hallucinations under psychedelics and in the 760 schizophrenia spectrum: An interdisciplinary and multiscale comparison, *Schizophrenia Bulletin* 46 (6) (2020) 1396–1408. doi:10.1093/schbul/sbaa117.

[21] R. A. Adams, Q. J. Huys, J. P. Roiser, Computational psychiatry: Towards a mathematically informed understanding of mental illness, *Journal of Neurology, Neurosurgery & Psychiatry* 87 (1) (2016) 53–63. 765

[22] P. C. Fletcher, C. D. Frith, Perceiving is believing: A Bayesian approach to explaining the positive symptoms of schizophrenia, *Nature Reviews Neuroscience* 10 (1) (2009) 48–58.

[23] W. J. Speechley, J. C. Whitman, T. S. Woodward, The contribution of hypersalience to the “jumping to conclusions” bias associated with delusions in schizophrenia, *Journal of Psychiatry & Neuroscience: JPN* 35 (1) (2010) 7. 770

[24] R. A. Adams, K. E. Stephan, H. R. Brown, C. D. Frith, K. J. Friston, The computational anatomy of psychosis, *Frontiers in Psychiatry* 4 (2013) 47.

[25] S. Brugger, M. Broome, Computational psychiatry, in: *The Routledge Handbook of the Computational Mind*, Routledge, 2018, pp. 452–468. 775

[26] R. L. Carhart-Harris, K. Friston, REBUS and the anarchic brain: Toward a unified model of the brain action of psychedelics, *Pharmacological Reviews* 71 (3) (2019) 316–344.

[27] C. A. Tamminga, E. I. Ivleva, M. S. Keshavan, G. D. Pearlson, B. A. Clementz, B. Witte, D. W. Morris, J. Bishop, G. K. Thaker, J. A. Sweeney, Clinical phenotypes of psychosis in the bipolar-schizophrenia network on intermediate phenotypes (b-snip), *American Journal of psychiatry* 170 (11) (2013) 1263–1274. 780

[28] S. D. Muthukumaraswamy, A. D. Shaw, L. E. Jackson, J. Hall, R. Moran, N. Saxena, Evidence that subanesthetic doses of ketamine cause sustained disruptions of NMDA and AMPA-mediated frontoparietal connectivity in humans, *Journal of Neuroscience* 35 (33) (2015) 11694–11706.

[29] R. Oostenveld, P. Fries, E. Maris, J.-M. Schoffelen, Fieldtrip: Open source software for advanced analysis of MEG, EEG, and invasive electrophysiological data, *Computational Intelligence and Neuroscience* 2011 (2011) 1:1–1:9. doi:10.1155/2011/156869.

[30] A. Delorme, S. Makeig, EEGLAB: An open source toolbox for analysis of single-trial EEG dynamics including independent component analysis, *Journal of Neuroscience Methods* 134 (1) (2004) 9–21. doi:10.1016/j.jneumeth.2003.10.009.

[31] I. Winkler, S. Haufe, M. Tangermann, Automatic classification of artifactual ica-components for artifact removal in eeg signals, *Behavioral and Brain Functions* 7 (1) (2011) 1–15.

[32] B. D. Van Veen, W. Van Dronkelaar, M. Yuchtman, A. Suzuki, Localization of brain electrical activity via linearly constrained minimum variance spatial filtering, *IEEE Transactions on Biomedical Engineering* 44 (9) (1997) 867–880.

[33] N. Tzourio-Mazoyer, B. Landeau, D. Papathanassiou, F. Crivello, O. Etard, N. Delcroix, B. Mazoyer, M. Joliot, Automated anatomical labeling of activations in SPM using a macroscopic anatomical parcellation of the MNI MRI single-subject brain, *NeuroImage* 15 (1) (2002) 273–289.

[34] T. Bossomaier, L. Barnett, M. Harré, J. T. Lizier, *An Introduction to Transfer Entropy*, Vol. 65, Springer, 2016.

[35] T. Andrillon, A. T. Poulsen, L. K. Hansen, D. Léger, S. Kouider, Neural markers of responsiveness to the environment in human sleep, *Journal of Neuroscience* 36 (24) (2016) 6583–6596. doi:10.1523/JNEUROSCI.0902-16.2016.

[36] X.-S. Zhang, R. J. Roy, E. W. Jensen, EEG complexity as a measure of depth of anesthesia for patients, *IEEE Transactions on Biomedical Engineering* 48 (12) (2001) 1424–1433. doi:10.1109/10.966601.

[37] D. Dolan, H. J. Jensen, P. A. Mediano, M. Molina-Solana, H. Rajpal, F. Rosas, J. A. Sloboda, The improvisational state of mind: A multidisciplinary study of an improvisatory approach to classical music repertoire performance, *Frontiers in Psychology* 9 (2018) 1341. doi:10.3389/fpsyg.2018.01341.

[38] F. Kaspar, H. Schuster, Easily calculable measure for the complexity of spatiotemporal patterns, *Physical Review A* 36 (2) (1987) 842. doi:10.1103/PhysRevA.36.842.

[39] J. Ziv, Coding theorems for individual sequences, *IEEE Transactions on Information Theory* (1978). doi:10.1109/TIT.1978.1055911.

[40] T. M. Cover, J. A. Thomas, *Elements of Information Theory*, Wiley, Hoboken, 2006.

[41] L. Barnett, A. B. Barrett, A. K. Seth, Granger causality and transfer entropy are equivalent for Gaussian variables, *Physical Review Letters* 103 (23) (2009) 238701. doi:10.1103/physrevlett.103.238701.

[42] G. Deco, D. Vidaurre, M. L. Kringelbach, Revisiting the global workspace orchestrating the hierarchical organization of the human brain, *Nature Human Behaviour* 5 (4) (2021) 497–511. doi:10.1038/s41562-020-01003-6.

[43] L. Barnett, A. K. Seth, Granger causality for state-space models, *Physical Review E* 91 (4) (2015) 040101. doi:10.1103/PhysRevE.91.040101.

[44] L. Barnett, A. K. Seth, The MVGC multivariate Granger causality toolbox: A new approach to Granger-causal inference, *Journal of Neuroscience Methods* 223 (2014) 50–68. doi:10.1016/j.jneumeth.2013.10.018.

[45] N. Gauvrit, H. Zenil, F. Soler-Toscano, J.-P. Delahaye, P. Brugger, Human behavioral complexity peaks at age 25, *PLoS Computational Biology* 13 (4) (2017) e1005408. doi:10.1371/journal.pcbi.1005408.

[46] A. Zalesky, A. Fornito, E. T. Bullmore, Network-based statistic: Identifying differences in brain networks, *NeuroImage* 53 (4) (2010) 1197–1207.

[47] S. J. Gershman, What does the free energy principle tell us

800 about the brain?, *Neurons, Behavior, Data analysis, and Theory* (2019).

[48] P. Sterzer, R. A. Adams, P. Fletcher, C. Frith, S. M. Lawrie, L. Muckli, P. Petrovic, P. Uhlhaas, M. Voss, P. R. Corlett, The predictive coding account of psychosis, *Biological psychiatry* 84 (9) (2018) 634–643.

[49] C. Teufel, N. Subramaniam, V. Dobler, J. Perez, J. Finnemann, P. R. Mehta, I. M. Goodyer, P. C. Fletcher, Shift toward prior knowledge confers a perceptual advantage in early psychosis and psychosis-prone healthy individuals, *Proceedings of the National Academy of Sciences* 112 (43) (2015) 13401–13406.

[50] P. R. Corlett, G. Horga, P. C. Fletcher, B. Alderson-Day, K. Schmack, A. R. Powers III, Hallucinations and strong priors, *Trends in cognitive sciences* 23 (2) (2019) 114–127.

[51] F. Schneider, F. Bermpohl, A. Heinzel, M. Rotte, M. Wallentin, C. Tempelmann, C. Wiebking, H. Dobrowolny, H. Heinze, G. Northoff, The resting brain and our self: self-relatedness modulates resting state neural activity in cortical midline structures, *Neuroscience* 157 (1) (2008) 120–131.

[52] R. Ratcliff, J. N. Rouder, Modeling response times for two-choice decisions, *Psychological Science* 9 (5) (1998) 347–356.

[53] P. Dayan, S. Kakade, P. R. Montague, Learning and selective attention, *Nature Neuroscience* 3 (11) (2000) 1218–1223.

[54] P. Dayan, A. Jyu, Uncertainty and learning, *IETE Journal of Research* 49 (2-3) (2003) 171–181.

[55] J. Durbin, S. J. Koopman, *Time Series Analysis by State Space Methods*, Oxford University Press, 2012.

[56] T. K. Moon, The expectation-maximization algorithm, *IEEE Signal Processing Magazine* 13 (6) (1996) 47–60.

[57] G. B. Keller, T. D. Mrsic-Flogel, Predictive processing: a canonical cortical computation, *Neuron* 100 (2) (2018) 424–435.

[58] P. Sterzer, A. L. Mishara, M. Voss, A. Heinz, Thought insertion as a self-disturbance: an integration of predictive coding and phenomenological approaches, *Frontiers in human neuroscience* 10 (2016) 502.

[59] C.-E. Notredame, D. Pins, S. Deneve, R. Jardri, What visual illusions teach us about schizophrenia, *Frontiers in integrative neuroscience* 8 (2014) 63.

[60] K. J. Friston, K. E. Stephan, R. Montague, R. J. Dolan, Computational psychiatry: the brain as a phantastic organ, *The Lancet Psychiatry* 1 (2) (2014) 148–158.

[61] R. Balzan, P. Delfabbro, C. Galletly, T. Woodward, Confirmation biases across the psychosis continuum: The contribution of hypersalient evidence-hypothesis matches, *British Journal of Clinical Psychology* 52 (1) (2013) 53–69.

[62] V. C. Leeson, T. W. Robbins, E. Matheson, S. B. Hutton, M. A. Ron, T. R. Barnes, E. M. Joyce, Discrimination learning, reversal, and set-shifting in first-episode schizophrenia: Stability over six years and specific associations with medication type and disorganization syndrome, *Biological Psychiatry* 66 (6) (2009) 586–593.

[63] J. A. Waltz, J. M. Gold, Probabilistic reversal learning impairments in schizophrenia: Further evidence of orbitofrontal dysfunction, *Schizophrenia Research* 93 (1-3) (2007) 296–303.

[64] S. M. Silverstein, B. P. Keane, Perceptual organization impairment in schizophrenia and associated brain mechanisms: review of research from 2005 to 2010, *Schizophrenia bulletin* 37 (4) (2011) 690–699.

[65] H. K. Horton, S. M. Silverstein, Visual context processing deficits in schizophrenia: effects of deafness and disorganization, *Schizophrenia bulletin* 37 (4) (2011) 716–726.

[66] G. Northoff, P. Qin, How can the brain's resting state activity generate hallucinations? a 'resting state hypothesis' of auditory verbal hallucinations, *Schizophrenia research* 127 (1-3) (2011) 202–214.

[67] G. Northoff, N. W. Duncan, How do abnormalities in the brain's spontaneous activity translate into symptoms in schizophrenia? from an overview of resting state activity findings to a proposed spatiotemporal psychopathology, *Progress in neurobiology* 145 (2016) 26–45.

[68] P. A. Mediano, F. E. Rosas, A. I. Luppi, R. L. Carhart-Harris, D. Bor, A. K. Seth, A. B. Barrett, Towards an extended taxonomy of information dynamics via Integrated Information Decomposition, *arXiv preprint arXiv:2109.13186* (2021).

[69] A. R. Powers, C. Mathys, P. R. Corlett, Pavlovian conditioning-induced hallucinations result from overweighting of perceptual priors, *Science* 357 (6351) (2017) 596–600.

[70] C. M. Cassidy, P. D. Balsam, J. J. Weinstein, R. J. Rosengard, M. Slifstein, N. D. Daw, A. Abi-Dargham, G. Horga, A perceptual inference mechanism for hallucinations linked to striatal dopamine, *Current Biology* 28 (4) (2018) 503–514.

[71] B. Alderson-Day, C. F. Lima, S. Evans, S. Krishnan, P. Shanmugalingam, C. Fernyhough, S. K. Scott, Distinct processing of ambiguous speech in people with non-clinical auditory verbal hallucinations, *Brain* 140 (9) (2017) 2475–2489.

[72] P. A. M. Mediano, F. E. Rosas, A. B. Barrett, D. Bor, Decomposing spectral and phasic differences in nonlinear features between datasets, *Physical Review Letters* 127 (12) (2021) 124101. doi:10.1103/PhysRevLett.127.124101.

[73] A. M. Bastos, J. Vezoli, C. A. Bosman, J.-M. Schoffelen, R. Oostenveld, J. R. Dowdall, P. De Weerd, H. Kennedy, P. Fries, Visual areas exert feedforward and feedback influences through distinct frequency channels, *Neuron* 85 (2) (2015) 390–401. doi:10.1016/j.neuron.2014.12.018.

[74] A. Brouwer, R. L. Carhart-Harris, Pivotal mental states, *Journal of Psychopharmacology* 35 (4) (2021) 319–352. doi:10.1177/0269881120959637.

[75] P. Mediano, A. Ikkala, R. A. Kievit, S. R. Jagannathan, T. F. Varley, E. A. Stamatakis, T. A. Bekinschtein, D. Bor, Fluctuations in neural complexity during wakefulness relate to conscious level and cognition, *bioRxiv* (2021). doi:10.1101/2021.09.23.461002.

[76] F. E. Turkheimer, F. E. Rosas, O. Dipasquale, D. Martins, E. D. Fagerholm, P. Expert, F. Váša, L.-D. Lord, R. Lee, A complex systems perspective on neuroimaging studies of behavior and its disorders, *The Neuroscientist* (2021) 1073858421994784 doi:10.1177/1073858421994784.